J Mater Sci (2015) 50:6757–6767
DOI 10.1007/s10853-015-9231-6

# Utilisation of cement-asbestos wastes by thermal treatment and the potential possibility use of obtained product for the clinker bricks manufacture

**Robert Kusiorowski[1,2] · Teresa Zaremba[1] · Jerzy Piotrowski[1] · Jacek Podwórny[2]**

Received: 7 April 2015 / Accepted: 2 July 2015 / Published online: 9 July 2015


**Abstract** The aim of this study was to investigate the thermal behaviour of cement-asbestos wastes and to determine whether it is possible to use them in the production of building ceramics, e.g. clinker bricks. In the first part of the research, the process of cement-asbestos thermal decomposition was studied. This asbestos material contained the chrysotile and crocidolite variety of asbestos. The results of this study allowed to determine the lowest temperature of thermal treatment that provides asbestos detoxification. The second part of the paper presents the results of a preliminary study on using previously calcined cement-asbestos wastes as an additive to ceramic masses typical for clinker bricks. Green compacts containing various amounts of cement-asbestos wastes were sintered and then ceramic properties were determined. The results of the study indicate that calcined asbestos-containing materials can be used as one of the secondary raw materials in the production of clinker ceramics.

## Introduction

Asbestos is the commercial name for several types of naturally occurring fibrous silicate minerals. These minerals are divided into two main groups: serpentine and amphibole asbestos. Serpentines are hydrous magnesium silicates and they occur as one asbestiform, fibrous mineral: chrysotile (white asbestos) with an ideal chemical formula, $Mg_3(OH)_4(Si_2O_5)$. This mineral with sheet structure was the most often commercially used form of asbestos and covered more than 90 % of world production of asbestos. Amphiboles are double-chain silicates and contain five asbestiform minerals with an ideal chemical formula: actinolite $Ca_2(Mg,Fe)_5[(OH)Si_4O_{11}]_2$, amosite $(Fe,Mg)_7[(OH)Si_4O_{11}]_2$, anthophyllite $(Mg,Fe)_7[(OH)Si_4O_{11}]_2$, crocidolite $Na_2Fe_3Fe_2[(OH)Si_4O_{11}]_2$, and tremolite $Ca_2Mg_5[(OH)Si_4O_{11}]_2$. Among these amphibole minerals, only crocidolite (blue asbestos) and amosite (brown asbestos) were used on a large industrial scale [1, 2].

Due to the preferred usable features such as non-flammability, mechanical and tensile strength, electrical, heat or sound insulating properties and chemical resistance, asbestos minerals were widely used in the past for various industrial applications. The main direction of asbestos use was the widely understood building industry. The most popular products based on asbestos were cement-asbestos assortments. About 85 % of asbestos imported to Poland was used for their production [3]. The huge popularity of cement-asbestos in the building industry of the twentieth century stemmed from its inexpensive production process combined with ease of forming various shapes. The most extensive use has been in flat sheets, tiles, corrugated sheets for roofing, rainwater and pressure pipes. Cement-asbestos products usually contained 10–16 wt% of asbestos, whose main function was fibrous reinforcement in the cement [4].

Generally, the asbestos era ended in developed countries in the late twentieth century when the carcinogenic properties of asbestos were discovered and confirmed by many studies. On the other hand, it should also be noted that there

✉ Robert Kusiorowski
r.kusiorowski@icimb.pl; robert.kusiorowski@interia.pl

[1] Department of Inorganic, Analytical Chemistry and Electrochemistry, Faculty of Chemistry, Silesian University of Technology, B. Krzywoustego Str. 6, 44-100 Gliwice, Poland

[2] Refractory Materials Division in Gliwice, Institute of Ceramics and Building Materials, Toszecka Str. 99, 44-100 Gliwice, Poland

are still countries where the manufacture and use of asbestos-containing materials is not prohibited [5]. Currently, asbestos minerals are considered as hazardous material for people that cause lung diseases such as asbestosis or lung cancer. The most dangerous are the respirable fibres, which have a length greater than 5 μm, a diameter less than 3 μm and a length-to-diameter ratio above 3:1 [6, 7]. In many countries there is only one way of dealing with these dangerous wastes, which are stored in controlled landfill sites [8]. This procedure does not completely solve the asbestos problem because the fibrous structure of asbestos is not destroyed—it is only isolated from the human environment.

In the literature there are several reports about possible utilisation methods of asbestos- containing materials which generally describe the destruction of the asbestos fibrous structure by dissolution in an acidic environment [9–12], melting and subsequent solidification [13–15], amorphisation by mechanochemical techniques [16, 17], or by biological method [18]. Asbestos-containing wastes can also be subject to classic heat treatment (calcination, annealing) at a sufficiently high temperature, providing thermal decomposition of asbestos minerals. The last method is most commonly presented in the specialist literature [19–22] because of its simplicity in implementation and potentially wide range of proposed applications of the obtained product after thermal treatment, e.g. as secondary ceramic raw material [23–26].

The thermal utilisation method of asbestos minerals is quite well known, especially with respect to chrysotile asbestos, and has been described in the specialist literature [27–30]. Generally, this method is associated with the dehydroxylation process of asbestos minerals and in designating the optimal temperature of thermal treatment. In the case of cement-asbestos materials, these investigations can be more complicated due to the multiphase reacting system. The reaction paths should be completely modified due to the presence of other cementitious phases and operating conditions, e.g. varying degrees of exposure to weather conditions in which the cement-asbestos assortment was used [31–33].

Important results were provided in a study by Italian researchers [34] who studied more than 25 cement-asbestos samples removed from different locations in Italy. Chemical analysis of the tested samples showed significant differences in the chemical composition (expressed as oxides); for example, the content of $SiO_2$ ranged from 21.8 to 45.2 wt%, while the CaO content changed from 26.7 to 38.4 wt%. Other components were also changed to a lesser or greater extent. Phase composition as determined by the X-ray analysis method was also varied. Generally, among all of the tested samples the authors identified 25 different crystalline phases. In aged cement-asbestos samples, calcite was the most abundant detected crystalline phase. On the other hand, the weight fraction of the amorphous fraction not determined by XRD analysis was quite variable and ranged from 9.5 to 66.6 wt%. Chrysotile asbestos was identified in all samples, while amphibole asbestos (without distinction as to the type of amphibole asbestos) was detected in 17 out of 29 samples. The authors also identified products of cement hydration and unreacted clinker phases. According to the authors, batches of cement-asbestos materials from different plants, in particular slates and undergoing the same thermal treatment, may yield different end products. This was confirmed by studies presented by Viani et al. [35], in which the high-temperature inertisation product of a representative batch of previously mentioned cement-asbestos samples was characterised. The chemistry of the investigated samples is dominated by Si, Ca and Mg, although significant differences between the samples exist. All of the raw cement-asbestos samples were heated at 1200 °C for 15 min and then were characterised with a combination of analytical techniques. A series of solid state reactions leading to global structural changes of the matrix with a complete transformation of asbestos minerals was observed. After thermal treatment, phase composition was determined by XRD analysis in which the authors found about 25 crystalline phases in the cement-asbestos materials in various proportions depending on the origin of the cement-asbestos waste. The authors identified three classes of product obtained by high-temperature cement-asbestos treatment. They indicated that the obtained material may belong to a larnite-rich, bredigite-rich or akermanite-rich product and hence can find various further applications.

The aim of the research presented in this study was (i) to determine thermal stability as well as structural and phase changes of cement-asbestos corrugated sheet during the calcination process to a high temperature and to classify it into one of the above-mentioned classes (ii) to select the minimal temperature of cement-asbestos thermal treatment at which the dangerous properties of asbestos disappeared, and (iii) to demonstrate the possibility of using previously thermally treated cement-asbestos material as a secondary raw material in the manufacture of clinker ceramics used as a building material.

## Experimental

The subject of examination was corrugated cement-asbestos slate. The slate came from Upper Silesia (Poland), from around the city of Mikołów. The slate had been exposed to outside weather conditions for about 30 years. The asbestos material was the façade and roof panels of a shed. Different types of asbestos were observed in the

fracture of a sample, e.g. there were yellowish-green and dark-blue bundles of fibres, potentially chrysotile and crocidolite asbestos, respectively. This cement-asbestos material was subjected to classical wet chemical analysis and the main chemical components were determined by standard laboratory procedure applied for the chemical analysis of aluminosilicate materials. The cement-asbestos sample was fused with a mixture of sodium carbonate and sodium tetraborate, evaporated to dryness with concentrated hydrochloric acid for isolation of silicic acid anhydride and then filtered and calcined for the resulting precipitate. The resulting filtrate was used for further assays for which $Fe_2O_3$, $Al_2O_3$, CaO and MgO contents were determined by titration with EDTA (ethylenediaminetetraacetic acid sodium salt complexing agent) against appropriate indicators. The $SiO_2$ content was determined using the gravimetric method by stripping silicic acid anhydride using hydrofluoric acid. The $SO_3$ content was also determined gravimetrically by dissolving the sample in hydrochloric acid and following precipitation of sulphate ions by barium ions. Loss on ignition (LOI) was determined by annealing in a laboratory oven at 1000 °C to a constant weight.

This cement-asbestos waste was subjected to ex situ X-ray analysis (XRD), Fourier transform infrared spectroscopy (FT-IR) as well as differential thermal analysis (DTA) and thermogravimetry (TG). Moreover, its microstructure was observed by scanning electron microscopy (SEM). In order to accurately determine the temperature range of the disappearance of asbestos mineral by thermal treatment and change in phase composition, high-temperature X-ray measurement (in situ method; HT-XRD) was applied. The minimal temperature of cement-asbestos thermal treatment was selected based on the obtained results. Then, to check for potential usability of cement-asbestos waste as a secondary raw material for the production of clinker ceramics, the waste was subjected to initial calcination in a laboratory furnace at a selected temperature for 2 h. The obtained product was also characterised by XRD, FT-IR, DTA/TG and SEM analysis.

Thermal analysis (DTA and TG) was performed using a Paulik–Paulik–Erdey type derivatograph (MOM, Hungary) within the range of temperature of 20–1000 °C. The conditions were as follows: mass of sample 500 mg, air atmosphere, heating rate 10 K $min^{-1}$, alumina crucible and $Al_2O_3$ as the reference material. XRD analysis of the examined samples was carried out using a PANalytical X'pert Pro diffractometer ($CuK_\alpha$ radiation, Ni filter, 40 kV, 30 mA, X'Celerator detector). The in situ high-temperature diffraction experiment was conducted using the same diffractometer equipped with an Anton Paar HTK2000 heating chamber. X-ray diffraction patterns were collected in continuous mode in a range of 6°–55° $2\theta$. Data were collected in the temperature range of 25–1200 °C, at steps of 100 °C with additional measurement at 650 °C. IR-spectra were measured on a Nicolett 6700 FT-IR spectrophotometer (ATR method). The microstructure of the samples was examined by a scanning electron microscope (Hitachi TM-3000). Observations were made after coating the sample surfaces with a thin layer of gold in order to obtain conductivity.

A commercial raw mix of ceramic clinker was used (CRH Klinkier; Patoka, Poland) in the second stage of the study during which recycling tests were carried out. The chemical composition of used commercial raw mix of ceramic clinker is as follows: $SiO_2$ 62.4 wt%, $Al_2O_3$ 17.0 wt%, $Fe_2O_3$ 9.5 wt%, $TiO_2$ 0.8 wt%, CaO 0.4 wt%, MgO 1.3 wt%, $K_2O$ 2.0 wt%, MnO 0.2 wt%, LOI 6.3 wt%. Mineral composition of used commercial raw mix contains clay and non-clay minerals. Among clay minerals a principal role is played by kaolinite (ICDD-PDF 00-058-2028). Illite (ICDD-PDF 00-026-0911) is present as an admixture. Non-clay minerals are represented by quartz (ICDD-PDF 01-070-3755), muscovite (ICDD-PDF 01-070-3754) and siderite (ICDD-PDF 00-029-0696).

Different amounts of previously calcined cement-asbestos (0–10 wt%) were added as a leaning agent, i.e. a component that reduces shrinkage, to this mass. The raw materials had the following grain size: <1 mm for clay and <0.5 mm for calcined cement-asbestos. The mixtures were homogenised in a ball-mill for 15 min, then mixing water was added (15 wt% to obtain semi-dry masses) and further homogenised for 24 h in a closed foil bag. The green samples, formed as cylinders (30 mm in diameter and about 30 mm in height, uniaxial compression at 15 MPa), were dried in room temperature and in a laboratory dryer at 105 °C. Then they were sintered at 1100, 1150 and 1200 °C for 1 h at maximum temperature. Finally, these samples were naturally cooled in a furnace until they reached room temperature. After thermal treatment, total linear shrinkage, water absorption, open porosity, apparent density and compressive strength were measured on representative samples following standard laboratory procedures. Freeze resistance was also determined.

## Results and discussion

### Characterisation of the cement-asbestos material and its thermal decomposition

The chemical composition of the investigated cement-asbestos sample is reported in Table 1. These values are close to the results obtained in a chemical analysis by Witek et al. [36], where the content of the main chemical components was as follows: CaO 41.8 wt%, $SiO_2$ 19.3 wt%

**Table 1** Main chemical components of cement-asbestos waste

| Item | Content (wt%) |
|---|---|
| $SiO_2$ | 18.5 |
| CaO | 41.9 |
| MgO | 3.7 |
| $Al_2O_3$ | 2.7 |
| $Fe_2O_3$ | 3.4 |
| $SO_3$ | 1.9 |
| LOI | 25.5 |

*LOI* loss on ignition

and LOI 25.1 wt%. Generally, the composition is also similar to that in samples tested by Viani et al. [34]. Values of the $SO_3$ and MgO content and loss on ignition are in the range reported by the Italian study [34]. In the considered cement-asbestos sample, the $SiO_2$ content is slightly smaller than the minimal participation in the Italian samples (18.5 vs. 21.8 wt%), while the CaO content is the biggest (41.9 vs. the 26.7–38.4 wt% range reported in [34]). This difference may be due to the different manufacturing processes of cement-asbestos and the ageing process, with varying intensity depending on the region and the time during which the cement-asbestos materials were used. According to [34], quartz was often used as a filler in Italian cement-asbestos products. Cement-asbestos manufacturers in Poland rather did not use additional mineral fillers. In the tested sample an increased content of $Fe_2O_3$ (3.4 vs. 2.9 wt% [36]) was also observed. This can be explained by the presence of crocidolite (blue asbestos) which increased the iron content in the sample.

Figure 1 shows the XRD patterns of the raw cement-asbestos sample and that calcined at a selected temperature (700 °C). This raw cement-asbestos sample contained both chrysotile (ICDD-PDF 00-027-1276) and crocidolite (ICDD-PDF 00-060-0343) asbestos. This is confirmed by the two strongest diffraction interferences originating from these asbestos minerals at 11°–12° $2\theta$. It can be observed that the main crystalline phases of raw cement-asbestos waste were calcium carbonate $CaCO_3$ (as calcite and vaterite (ICDD-PDF 04-012-8072, ICDD-PDF 00-060-0483, respectively)) and portlandite $Ca(OH)_2$ (ICDD-PDF 04-006-9147). Ettringite (ICDD-PDF 00-041-1451) and gypsum (ICDD-PDF 04-009-3817) as well as β-dicalcium silicate (ICDD-PDF 01-083-0461), tricalcium silicate (ICDD-PDF 04-014-9801), katoite (ICDD-PDF 00-038-0368) and traces of quartz (ICDD-PDF 00-033-1161) were also identified. Portlandite is one of the main products of the cement hydration process where the formation of calcium silicate hydrates (CSH phase) also occurs. The CSH phases generally possess a low degree of crystallinity and are X-ray amorphous, so they are rather not visible on the XRD patterns. In this cement-asbestos sample study, only the hydrogarnet of the katoite-hibschite series $Ca_3Al_2(SiO_4)_{3-x}(OH)_{4x}$ is the best represented and detected hydrated crystalline phase. Calcium carbonates are the main products of weathering as observed in the cement-asbestos sample. Their presence is due to the carbonation process of the cement matrix with atmospheric $CO_2$. Gypsum and ettringite are observed because gypsum $CaSO_4{\cdot}2H_2O$ was added as the setting-time regulator for cement and because they may be created as a result of interaction with the environment (acid rain). In the presence of gypsum the calcium aluminate of cement clinker reacts with water, producing ettringite $Ca_6Al_2(SO_4)_3(OH)_{12}{\cdot}26H_2O$. β-dicalcium silicate and tricalcium silicate were observed as unreacted clinker phases of cement.

Figure 2 shows the results of the in situ diffraction experiments (HT-XRD). From a technological point of view and with regard to the potential for thermal utilisation of cement-asbestos waste, the temperature range in which the diffraction interferences of asbestos minerals disappear is the most important. Due to the presence of two asbestos minerals in the considered sample (chrysotile and crocidolite), the absence of X-ray peaks of both types of asbestos is required. The obtained results show that with an increase in temperature the strongest asbestos diffraction interferences disappear at about 700 °C, which is marked as a loop in Fig. 2. Figure 3 was created based on HT-XRD measurement and reports the field of stability of all original and newly formed crystalline phases in the considered cement-asbestos sample with an increase in temperature to a maximum firing temperature of 1200 °C. The first phases to decompose are ettringite and katoite, with loss of water up to a temperature of 100 °C. According to [37], ettringite begins losing water at 70 °C and the short-range order in the crystal structure is disrupted. The thermal treatment product of ettringite becomes XRD-amorphous. In a temperature range of 100–200 °C, the presence of gypsum disappeared. Gypsum decomposed to anhydrite according to the reaction: $CaSO_4{\cdot}2H_2O \rightarrow CaSO_4{\cdot}1/2H_2O + 3/2H_2O \rightarrow CaSO_4 + 1/2H_2O$. The thermal decomposition products of katoite and gypsum are not visible on the XRD patterns, most probably due to poor crystallinity and low content in the obtained material after thermal treatment. Between 400 and 500 °C, subsequent phases of the cementitious matrix undergo a thermal transformation. In this temperature range portlandite decomposes according to the reaction: $Ca(OH)_2 \rightarrow CaO + H_2O$; vaterite is also converted to calcite. According to the literature [38], at a temperature of ~460 °C vaterite was subjected to the vaterite-calcite phase transition. Most interesting are the conclusions regarding asbestos stability. Both of the tested asbestos minerals, i.e. chrysotile and crocidolite, from the used cement-asbestos slate are stable up to a temperature of 600 °C. After measurement at a temperature of about

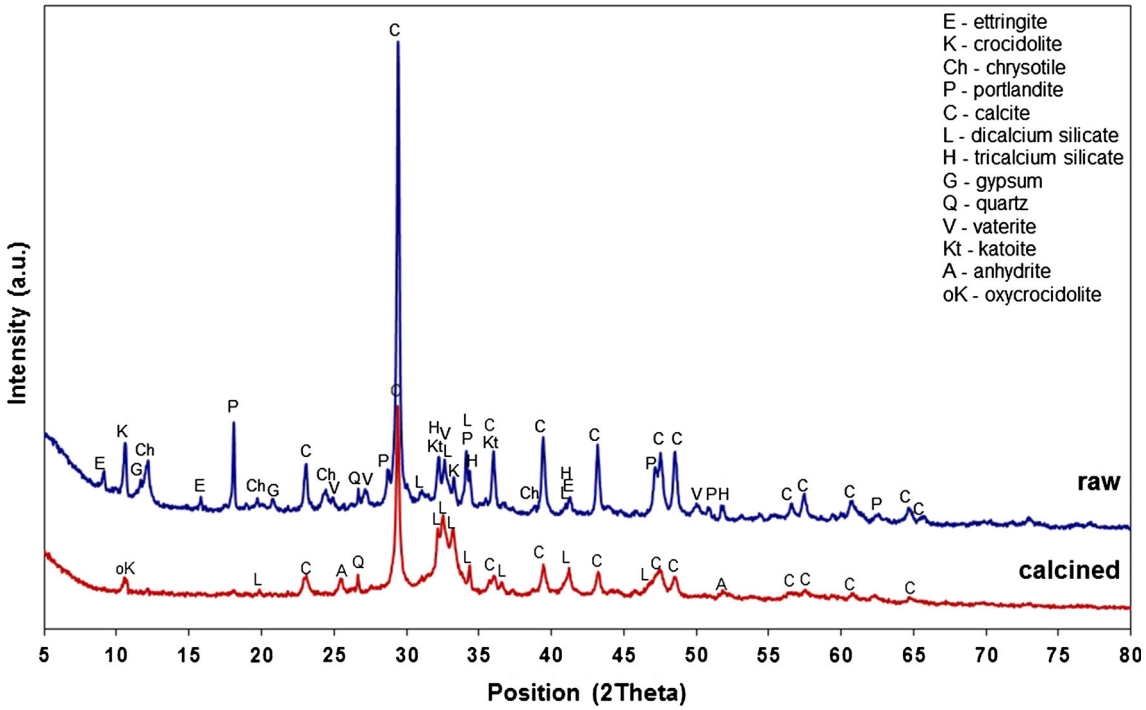


**Fig. 1** XRD patterns of raw cement-asbestos sample and after thermal treatment at 700 °C for 2 h

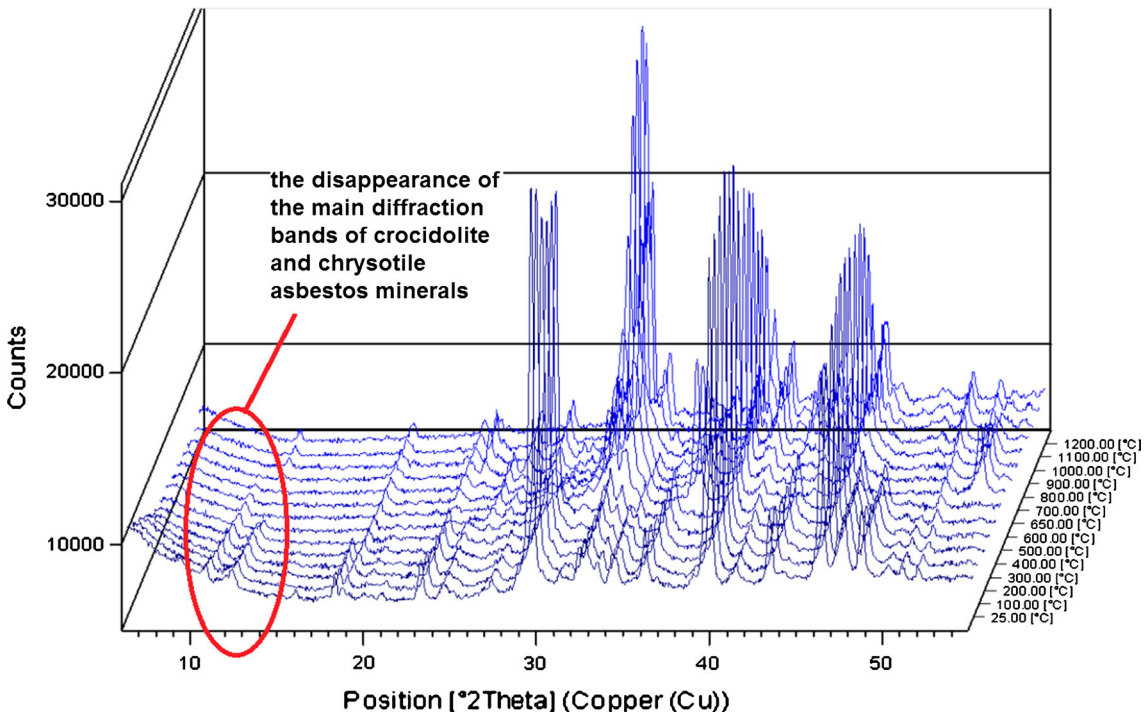


**Fig. 2** HT-XRD patterns of cement-asbestos sample

800 °C the chrysotile diffraction interferences were already absent (specific interferences disappear at 650 °C), while for crocidolite asbestos only slightly marked traces were observed. It comes from so-called oxycrocidolite. This is pseudomorph of crocidolite asbestos after its thermal decomposition and dehydroxylation process. However, the temperature 700 °C is sufficient for the thermal decomposition of crocidolite, which was confirmed by previous

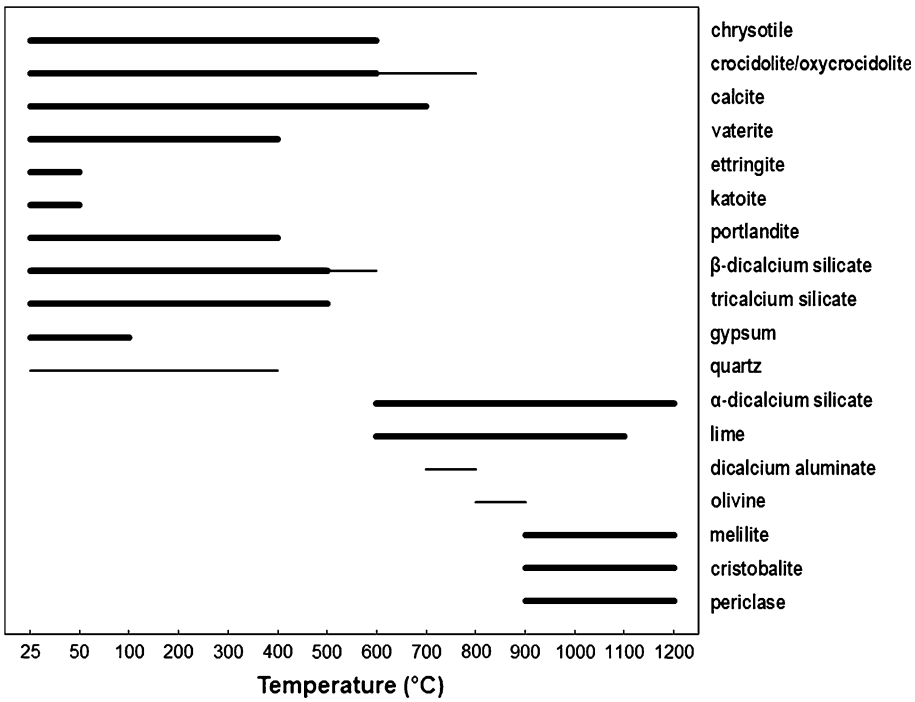


**Fig. 3** The temperature stability ranges of the crystalline phases in the cement-asbestos sample; narrow strip—traces of phase

studies [39], where was found that crocidolite asbestos undergoes dehydroxylation process in the temperature range 400–450 °C. Because the in situ diffraction experiment (HT-XRD) was carried out in dynamic conditions, this observation suggests that calcination of cement-asbestos at 700 °C should already be sufficient for thermal utilisation of asbestos-containing materials. As a result of asbestos minerals thermal decomposition at a higher temperature, traces of olivine $(Mg,Fe)_2SiO_4$ (ICDD-PDF 01-083-0648) were observed. Due to the presence of other phases from the cementitious matrix, products of asbestos thermal decomposition were incorporated into the new phases. Calcite decomposes ($CaCO_3 \rightarrow CaO + CO_2$) at about 700–800 °C and produces large amounts of CaO (ICDD-PDF 04-006-5940) which is available as a reactant for successive high-temperature reactions. Lime is present up to 1100 °C. The unreacted clinker phases of cement-like β-dicalcium silicate are stable up to 600 °C and are then transformed to the high-temperature variety ($\alpha$-$C_2S$ in cement notation, α-dicalcium silicate) [40]. After thermal treatment at 1200 °C, the periclase (ICDD-PDF 01-075-9568), cristobalite (ICDD-PDF 01-075-3164), dicalcium silicate (ICDD-PDF 00-031-0299) and melilite group $Ca_2(Mg,Fe,Al,Si)_3O_7$ (ICDD-PDF 04-016-3580) were observed.

Based on these results, a temperature of 700 °C was selected as a possible minimal value of firing treatment that provides thermal destruction of crocidolite and chrysotile asbestos contained in the cement-asbestos material that we tested. The main mineral components of thermally treated cement-asbestos material (after 2 h at 700 °C) were calcite and dicalcium silicate (Fig. 1). There were also no clearly visible diffraction interferences from the asbestos minerals. The weak interference at $\sim 11° \, 2\theta$ comes from a relic of crocidolite, so-called oxycrocidolite ($Na_2Fe_4FeSi_8O_{24}$), and is a result of the dehydroxylation process [41]. The external elongate crystal form is probably retained while the internal structure is already changed. This phenomenon is often observed in the case of clay minerals. It should be emphasised that, in accordance with [41], the dehydroxylation process of crocidolite asbestos occurs in a temperature range of 400–500 °C. This was confirmed by an infrared spectroscopy study. After this process, the crocidolite fibres lose their mechanical strength and are easy to crush [41].

The obtained product showed high grinding ability and was easily converted to pulverised shape material without any fibrous structures. This was confirmed by SEM observation (Fig. 4).The SEM micrograph of a cement-asbestos sample calcined at 700 °C and then lightly crushed shows no fibrous asbestos (Fig. 4c). Additional studies were carried out in order to confirm the selected minimal temperature of cement-asbestos calcination.

The results of differential thermal analysis (DTA) combined with thermogravimetric (TG) measurement of both raw and calcined cement-asbestos are reported in Fig. 5. On the DTA curve of raw cement-asbestos waste, four endothermic effects dominated which came from the decomposition of the cementitious matrix. All effects are connected with the mass change. Because of the small

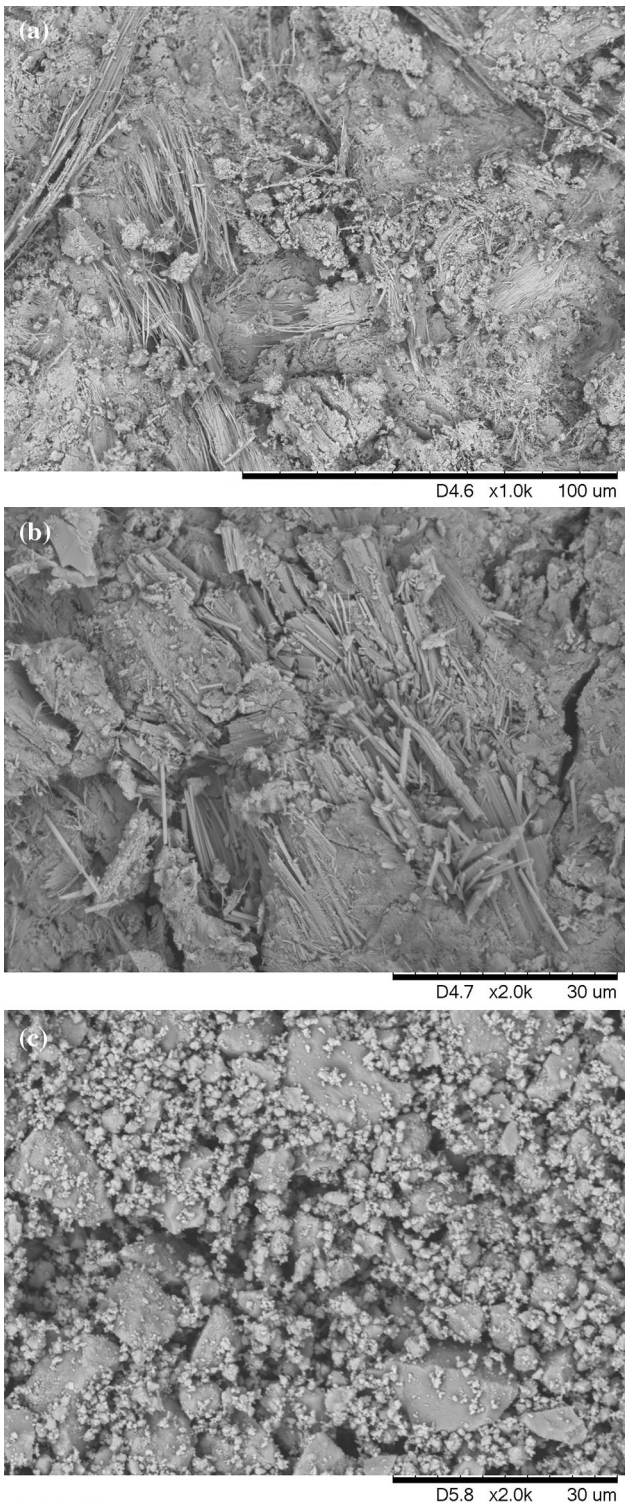


**Fig. 4** SEM images of the fracture of raw (**a**) cement-asbestos sample and after calcination at 700 °C for 2 h: unaffected (**b**) and after soft crush in agate mortar (**c**)

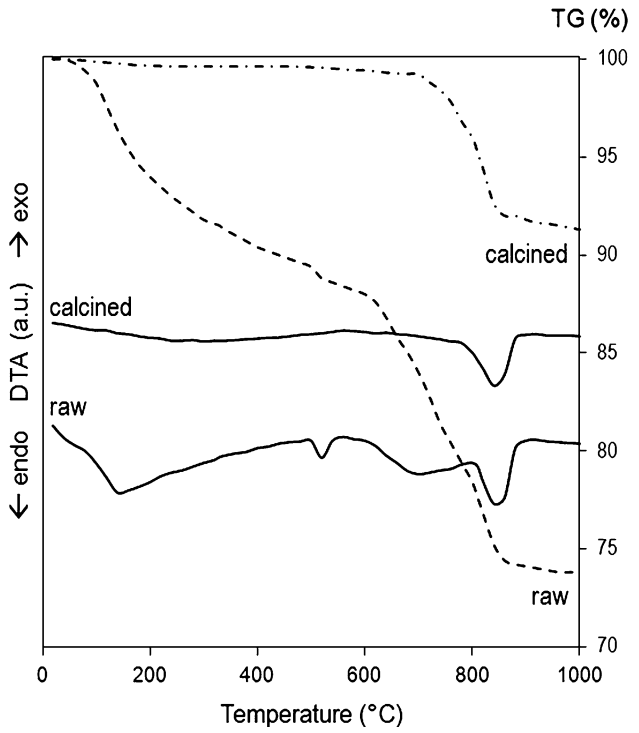


**Fig. 5** DTA and TG curves of raw cement-asbestos sample and after thermal treatment at 700 °C for 2 h

amount of asbestos minerals in the cement-asbestos material there were no visible characteristic effects from the decomposition of the identified asbestos minerals; these effects were masked by the thermal decomposition of the cementitious matrix components. The first wide endothermic peak is visible in a temperature range of 70–250 °C. This peak is connected mainly with water released from the CSH phase and AFt/AFm phase (i.e. ettringite and monosulfoaluminate) [42, 43]. The second endothermic peak at 520 °C indicates the presence of portlandite $Ca(OH)_2$ and its dehydroxylation ($Ca(OH)_2 \rightarrow CaO + H_2O$). In the wide temperature range of 650–800 °C, a third endothermic effect is observed. This wide temperature range of effect may indicate a different degree of crystallinity of the carbonate minerals [31] or the thermal decomposition of cementitious phases, e.g. jennite [44]. The normal single-step reaction of calcite thermal decomposition is gradually turned into a double-stage reaction by strong weathering conditions, whereas the calcite structure is disintegrated by the weathering process [45]. At a higher temperature (in the range of 800–900 °C) the decomposition of well-crystalline calcite ($CaCO_3$) takes place [46]. After isothermal calcination at 700 °C the most characteristic endothermic effects disappear. Only one effect was observed with a mass change in the range of 800–900 °C and indicated the presence and thermal decomposition of calcium carbonate ($CaCO_3 \rightarrow CaO + CO_2$).

To confirm the thermal decomposition of asbestos minerals included in the cement-asbestos material, sample obtained after calcination was studied by the FT-IR method

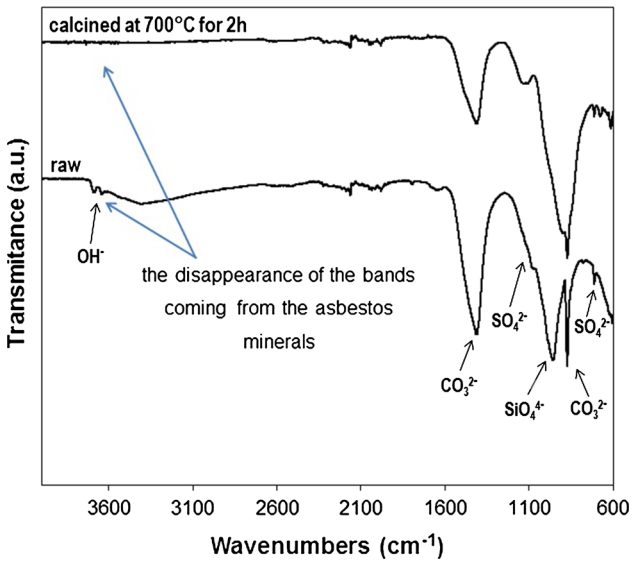


**Fig. 6** FT-IR spectra of raw cement-asbestos sample and after thermal treatment at 700 °C for 2 h

and compared with the IR spectrum of raw cement-asbestos. The results of this study are presented in Fig. 6. Absorbance bands related to the stretch of OH groups from asbestos minerals are visible on the FT-IR spectrum of the raw cement-asbestos sample in the high wavenumber region. The IR bands recorded in the region of 1400–1500 $cm^{-1}$ indicate the presence of carbonates and below 1100 $cm^{-1}$ are typical of the Si–O–Si stretches in the silica network. Calcination at 700 °C is sufficient for the asbestos transformation process which causes the disappearance of the characteristic absorption bands of asbestos minerals; the characteristic double band at 3640–3680 $cm^{-1}$ corresponding to the OH stretching vibrations of asbestos is lost. A characteristic carbonate band at $\sim$1400 $cm^{-1}$ remained due to the fact that the thermal treatment temperature was too low. A temperature of thermal treatment equal to 700 °C is too low for the complete thermal decomposition of calcite. This reaction is only initiated, which is indicated by lower intensity of the IR band.

## Recycling of the transformation product in clinker brick mixtures

In this section of the research previously calcined cement-asbestos (at 700 °C for 2 h) was used as a potential secondary raw material for the manufacture of clinker bricks. The results of the physical properties of the obtained clinker ceramic materials (Table 2) show that there is potential for the use of calcined cement-asbestos as a secondary raw material in the production of sintered ceramics.

The values of total linear shrinkage for the masses containing 5 wt% calcined cement-asbestos waste are at similar level to reference masses (without waste) for all sintering temperatures while those with 10 wt% shows lower values. The values of total linear shrinkage for these samples are generally decreased by $\sim$1 %. Moreover, with increase of the sintering temperature from 1150 to 1200 °C, for all ceramic masses, the inconsiderable decrease of values of this property are observed. It may indicate the initiation of the swelling process and exceeding the optimum firing conditions of ceramics. Confirmation of this fact may be practically no change in the values of apparent density between the samples sintered at 1150 and 1200 °C.

Water absorption as well as open porosity of the ceramic materials obtained on the basis of asbestos materials is generally higher than for comparative samples without any add-on cement-asbestos. The exception is material obtained with 5 wt% of calcined cement-asbestos and sintered at 1200 °C. In this case lower water absorption was obtained in comparison to the reference material (2.7 vs. 3.3 %). Also, the value of open porosity was the lowest

**Table 2** Properties of obtained clinker ceramics based on previously calcined (at 700 °C for 2 h) cement-asbestos

| Cement-asbestos content (%) | Mixing water (%) | Firing temperature (°C) | Total linear shrinkage (%) | Water absorption (%) | Open porosity (%) | Apparent density ($g/cm^3$) | Compressive strength (MPa) | Freeze resistance |
|---|---|---|---|---|---|---|---|---|
| 0 | 14.5 | 1100 | 7.1 | 5.0 | 11.3 | 2.28 | 35 | Full |
| | | 1150 | 7.8 | 3.8 | 8.6 | 2.30 | 37 | Full |
| | | 1200 | 7.6 | 3.3 | 7.6 | 2.30 | 41 | Full |
| 5 | 15.4 | 1100 | 7.1 | 5.9 | 13.8 | 2.19 | 26 | Full |
| | | 1150 | 7.8 | 5.2 | 11.5 | 2.21 | 31 | Full |
| | | 1200 | 7.3 | 2.7 | 6.0 | 2.21 | 35 | Full |
| 10 | 15.9 | 1100 | 6.2 | 8.3 | 17.7 | 2.13 | 25 | Full |
| | | 1150 | 6.7 | 7.3 | 15.8 | 2.15 | 31 | Full |
| | | 1200 | 6.1 | 3.9 | 8.4 | 2.16 | 39 | Full |

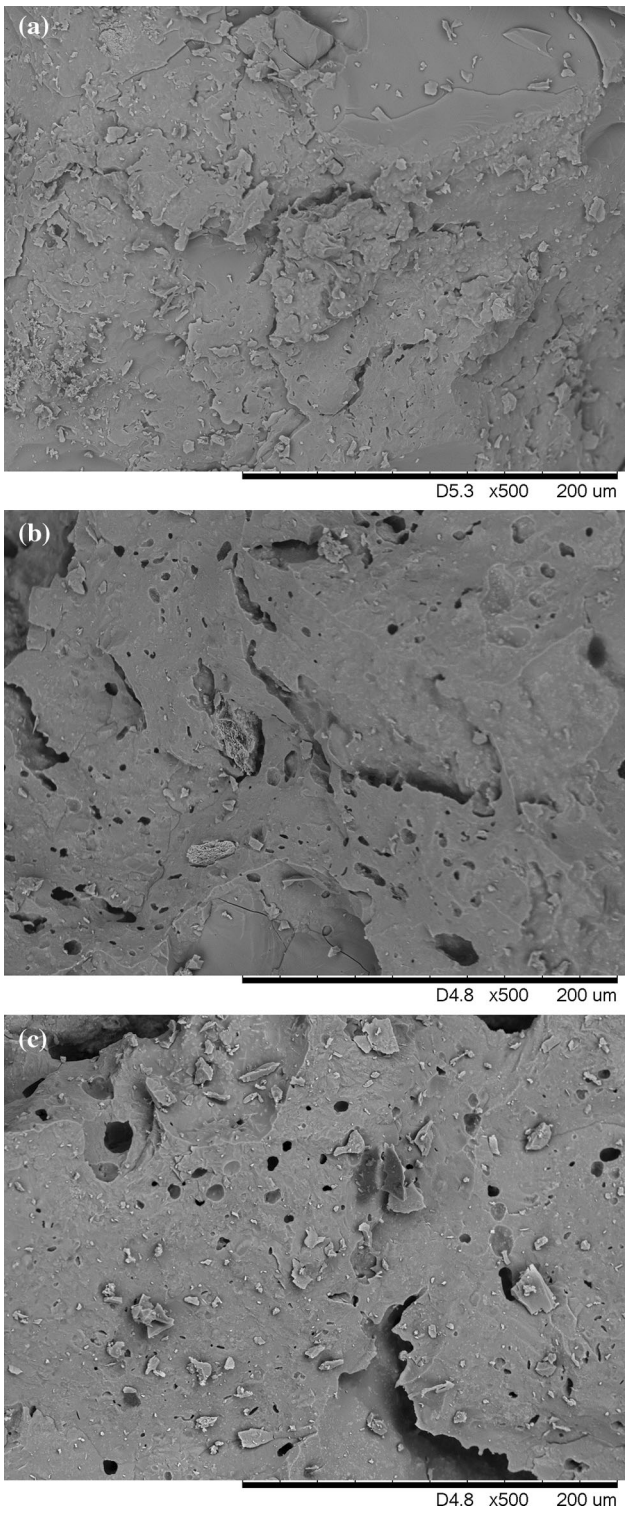


**Fig. 7** SEM microphotograph (fracture) of obtained clinker ceramic sintered at 1200 °C with different amounts of calcined cement-asbestos: 0 wt% (**a**), 5 wt% (**b**) and 10 wt% (**c**)

(6 %). Considering the values of water absorption, the most similar results were obtained for materials prepared with the smallest asbestos content, i.e. 5 wt%. The increase of cement-asbestos to 10 wt% in the ceramic mixtures visibly worsens water absorption. For each sintering temperature, the values of water absorption are higher in comparison to the reference clinker ceramics. However, it should be emphasised that the water absorption of clinker bricks, according to Polish industry standards (PN-B-12008:1996/Az1:2002), should not exceed 6 % and 10 % for building and road clinker, respectively. In the case of ceramic materials with calcined cement-asbestos addition the requirement for road clinker is fulfilled for each sintering temperature. When the sintering temperature is 1150–1200 °C for 5 wt% of cement-asbestos and 1200 °C for 10 wt% of calcined asbestos waste, the values of water absorption clearly fall below 6 % and the obtained ceramic material can be classified as building clinker ceramics.

The obtained results of compressive strength are also satisfactory. Compressive strength for clinker should be in the range of 22–75 MPa. The values of compressive strength for the obtained clinker ceramics with cement-asbestos were in the range of 25–40 MPa, thus the standard requirements are fulfilled. It should be noted that the addition of 10 wt% of cement-asbestos did not reduce the compressive strength of ceramic material as compared to the sample with 5 wt% of this waste. Moreover, for a sintering temperature of 1100 and 1150 °C the values are almost identical. The obtained ceramic materials have full freeze resistance, i.e. they can withstand 25 cycles of freezing and thawing in a temperature range from −25 °C to room temperature.

Characteristic microstructure images of the fracture of the obtained ceramic materials are shown in Fig. 7. A small amount of cement-asbestos (5 wt%) in the ceramic mixtures does not significantly influence the resulting ceramic materials as compared to materials without asbestos wastes. The SEM images are very similar. Increasing the cement-asbestos content to 10 wt% caused clear and visible differences in the microstructure of the resulting clinker brick material, which became more porous.

## Conclusions

Thermal treatment is one of the possible and useful methods of cement-asbestos detoxification. This study describes the reaction path and phase composition change that take place during the calcination of cement-asbestos slate containing chrysotile and crocidolite asbestos up to the thermal treatment temperature of 1200 °C. As a result of this process the dangerous structure of asbestos minerals is destroyed. The study showed that calcination of cement-asbestos (based on chrysotile and crocidolite variety of asbestos) at 700 °C is sufficient for thermal utilisation and that it contained absolutely no residual asbestos. The

obtained product has high grinding ability and is easily milled to pulverent material. In the second part of the research it was proved that thermally treated cement-asbestos at a temperature of 700 °C can be safely recycled as a secondary raw material in the manufacture of clinker ceramics. The addition of 5 wt% of calcined cement-asbestos material does not yield significant variations to the reference material and to the standard production parameters, e.g. water absorption, compressive strength or freeze resistance, of clinker bricks.



## References

1. Sporn TA (2011) Mineralogy of asbestos. In: Tannapfel A (ed) Malignant mesothelioma. Springer, Berlin, pp 1–11
2. Virta RL (2005) Mineral commodity profiles—Asbestos. U.S. Geological Survey Circular 1255-KK, Reston
3. Czekaj A, Dyczek J (2002) Korozja wyrobów azbestowo-cementowych i wynikające z niej ryzyko emisji azbestu (in Polish). Cement Wapno Beton 6:270–275
4. Bensted J, Smith JR (2011) Asbestos legacy impacts on future prospects. Cement Wapno Beton 3:161–166
5. LaDou J, Castleman B, Frank A, Gochfeld M, Greenberg M, Huff J, Joshi TK, Landrigan PJ, Lemen R, Myers J, Soffritti M, Soskolne CL, Takahashi K, Teitelbaum D, Terracini B, Watterson A (2010) The case for global ban on asbestos. Environ Health Perspect 118:897–901. doi:10.1289/ehp.1002285
6. Demirogiu H (1998) Hazard of white asbestos. Lancet 352:322–323. doi:10.1016/S0140-6736(05)60298-X
7. Langer AM (2003) Reduction of the biological potential of chrysotile asbestos arising from conditions of service on brake pads. Regul Toxicol Pharm 38:71–77. doi:10.1016/S0273-2300(03)00070-9
8. Dyczek J (2006) Eksploatacja i usuwanie wyrobów zawierających azbest (in Polish). Mater Bud 11:46–48
9. Sugama T, Sabatini R, Petrakis L (1998) Decomposition of chrysotile asbestos by fluorosulfonic acid. Ind Eng Chem Res 37:79–88. doi:10.1021/ie9702744
10. Turci S, Tomatis M, Mantegma S, Cravotto G, Fubini B (2007) The combination of oxalic acid with power ultrasound fully degrades chrysotile asbestos fibres. J Environ Monit 9:1064–1066. doi:10.1039/b709571f
11. Yanagisawa K, Kozawa T, Onda A, Kanazawa M, Shinohara J, Takanami T, Shiraishi M (2009) A novel decomposition technique of friable asbestos by $CHClF_2$-decomposed acidic gas. J Hazard Mater 163:593–599. doi:10.1016/j.jhazmat.2008.07.017
12. Rozalen M, Javier Huertas F (2013) Comparative effect of chrysotile leaching in nitric, sulfuric and oxalic acids at room temperature. Chem Geol 352:134–142. doi:10.1016/j.chemgeo.2013.06.004
13. Dellisanti F, Rossi PL, Valdre G (2009) Remediation of asbestos containing materials by Joule heating vitrification performed in a pre-pilot apparatus. Int J Miner Process 91:61–67. doi:10.1016/j.minpro.2008.12.001
14. Leonelli C, Veronesi P, Boccaccini DN, Rivasi MR, Barbieri L, Andreola F, Lancellotti I, Rabitti D, Pellacani GC (2006) Microwave thermal inertisation of asbestos containing waste and its recycling in traditional ceramics. J Hazard Mater B135:149–155. doi:10.1016/j.jhazmat.2005.11.035
15. Osada M, Takamiya K, Manako K, Noguchi M, Sakai S (2013) Demonstration study of high temperature melting for asbestos-containing waste (ACW). J Mater Cycles Waste Manag 15:25–36. doi:10.1007/s10163-012-0088-3
16. Plescia P, Gizzi D, Benedetti S, Camilucci L, Fanizza C, Simone De, Paglietti F (2003) Mechanochemical treatment to recycling asbestos–containing waste. Waste Manag 23:209–218. doi:10.1016/S0956-053X(02)00156-3
17. Colangelo F, Cioffi R, Lavorgna M, Verdolotti L, De Stefano L (2011) Treatment and recycling of asbestos-cement containing waste. J Hazard Mater 195:391–397. doi:10.1016/j.jhazmat.2011.08.057
18. Favero-Longo SE, Turci F, Tomatis M, Castelli D, Bonfante P, Hochella M, Piervittori R, Fubini B (2005) Chrysotile asbestos is progressively converted into a non-fibrous amorphous material by the chelating action of lichen metabolites. J Environ Monit 7:764–766. doi:10.1039/B507569F
19. Dellisanti F, Minguzzi V, Morandi N (2001–2002) Experimental results from thermal treatment of asbestos containing materials. GeoActa 1:61–70
20. Hashimoto S, Takeda H, Okuda A, Kamayashi A, Honda S, Iwamoto Fukuda K (2008) Detoxification of industrial asbestos waste by low-temperature heating in a vacuum. J Ceram Soc Jpn 116:242–246
21. Gualtieri AF, Lassinantti Gualtieri M, Tonelli M (2008) In situ ESEM study of the thermal decomposition of chrysotile asbestos in view of safe recycling of the transformation product. J Hazard Mater 156:260–266. doi:10.1016/j.jhazmat.2007.12.016
22. Kusiorowski R, Zaremba T, Piotrowski J, Gerle A (2013) Thermal decomposition of asbestos-containing materials. J Therm Anal Calorim 113:179–188. doi:10.1007/s10973-013-3038-y
23. Zaremba T, Peszko M (2008) Investigation of the thermal modification of asbestos wastes for potential use in ceramic formulation. J Therm Anal Calorim 92:873–877. doi:10.1007/s10973-007-8111-y
24. Gualtieri AF, Giacobbe C, Sardisco L, Saraceno M, Lassinantti Gualtieri M, Lusvardi G, Cavenati C, Zanatto I (2011) Recycling of the product of thermal inertization of cement-asbestos for various industrial applications. Waste Manag 31:91–100. doi:10.1016/j.wasman.2010.07.006
25. Zaremba T, Krząkała A, Piotrowski J, Garczorz D (2011) Investigations of chrysotile asbestos application for sintered ceramic obtaining. Mater Ceram 63:80–84
26. Zhu P, Wang LY, Hong D, Zhou M, Zhou J (2013) Investigative studies for inert transformation of toxic chrysotile tailing. J Mater Cycles Waste Manag 15:90–97. doi:10.1007/s10163-012-0093-6
27. Gualtieri AF, Tartaglia A (2000) Thermal decomposition of asbestos and recycling in traditional ceramics. J Eur Ceram Soc 20:1409–1418. doi:10.1016/S0955-2219(99)00290-3
28. Zaremba T, Krząkała A, Piotrowski J, Garczorz D (2010) Study on the thermal decomposition of chrysotile asbestos. J Therm Anal Calorim 101:479–485. doi:10.1007/s10973-010-0819-4
29. Kusiorowski R, Zaremba T, Piotrowski J, Adamek J (2012) Thermal decomposition of different types of asbestos. J Therm Anal Calorim 109:693–704. doi:10.1007/s10973-012-2222-9
30. Teixeira APC, Santos EM, Vieira AFP, Lago RM (2013) Use of chrysotile to produce highly dispersed K-doped MgO catalyst for biodiesel synthesis. Chem Eng J 232:104–110. doi:10.1016/j.cej.2013.07.065
31. Dias CMR, Cincotto MA, Savastano H, John VM (2008) Long-term aging of fiber-cement corrugated sheets—the effect of

carbonation, leaching and acid rain. Cem Concr Compos 30:255–265. doi:10.1016/j.cemconcomp.2007.11.001
32. Gualtieri AF, Cavenati C, Zanatto I, Meloni M, Elmi G, Lassinantti Gualtieri M (2008) The transformation sequence of cement-asbestos slates up to 1200 °C and safe recycling of the reaction product in stoneware tile mixtures. J Hazard Mater 152:563–570. doi:10.1016/j.jhazmat.2007.07.037
33. Belardi G, Piga L (2013) Influence of calcium carbonate on the decomposition of asbestos contained in end-of-life products. Thermochim Acta 573:220–228. doi:10.1016/j.tca.2013.08.019
34. Viani A, Gualtieri AF, Secco M, Peruzzo L, Artioli G, Cruciani G (2013) Crystal chemistry of cement-asbestos. Am Miner 98:1095–1105. doi:10.2138/am.2013.4347
35. Viani A, Gualtieri AF, Pollastri S, Rinaudo C, Croce A, Urso G (2013) Crystal chemistry of the high temperature product of transformation of cement-asbestos. J Hazard Mater 248–249:69–80. doi:10.1016/j.jhazmat.2012.12.030
36. Witek J, Mróz H, Barański J, Brach J (2012) Neutralisation of asbestos-containing waste using the method of melting in an arc-resistance furnace (in Polish). Sci Works Inst Ceram Build Mater 11:146–158
37. Antao SM, Duane MJ, Hassan I (2002) DTA, TG and XRD studies of sturmanite and ettringite. Can Miner 40:1403–1409. doi:10.2113/gscanmin.40.5.1403
38. Popescu MA, Isopescu R, Matei C, Fagarasan G, Plesu V (2014) Thermal decomposition of calcium carbonate polymorphs precipitated in the presence of ammonia and alkylamines. Adv Powder Technol 25:500–507. doi:10.1016/j.apt.2013.08.003
39. Kusiorowski R, Zaremba T, Gerle A, Piotrowski J, Simka W, Adamek J (2015) Study on the thermal decomposition of crocidolite asbestos. J Therm Anal Calorim 120:1585–1595. doi:10.1007/s10973-015-4421-7
40. Yamnova NA, Zubkova NV, Eremin NN, Zadov AE, Gazeev VM (2011) Crystal structure of larnite β-$Ca_2SiO_4$ and specific features of polymorphic transitions in dicalcium orthosilicate. Crystallogr Rep 56:210–220. doi:10.1134/S1063774511020209
41. Hodgson AA, Freeman AG, Taylor HFW (1965) The thermal decomposition of crocidolite from Koegas, South Africa. Miner Mag 35(269):5–30
42. Bădănoiu A, Paceagiu J, Voicu G (2011) Hydration and hardening processes of Portland cements obtained from clinkers mineralized with fluoride and oxides. J Therm Anal Calorim 103:879–888. doi:10.1007/s10973-010-1125-x
43. Perez-Rodriguez JL, Duran A, Perez-Marqueda LA (2011) Thermal study of unaltered and altered dolomitic rock samples from ancient monuments. J Therm Anal Calorim 104:467–474. doi:10.1007/s10973-011-1348-5
44. Stepkowska ET, Blanes JM, Real C, Perez-Rodriguez JL (2004) Phase transformation on heating of an aged cement paste. Thermochim Acta 420:79–87. doi:10.1016/j.tca.2003.11.05
45. Földvári M (2011) Handbook of thermogravimetric system of minerals and its use in geological practice. Geological Institute of Hungary, Budapest
46. Pacewska B, Wilińska I, Nowacka M (2011) Studies on the influence of different fly ashes and Portland cement on early hydration of calcium aluminate cement. J Therm Anal Calorim 106:859–868. doi:10.1007/s10973-011-1570-1